Communications Materials

https://doi.org/10.1038/s43246-026-01318-3

Article in Press

Slippery hydrophilic radiative cooling surfaces for optimal dew condensation and collection

Received: 16 September 2024

Accepted: 29 July 2026

Published online: 05 August 2026

Cite this article as: Huang, X., Wu, S., Mandal, J. *et al.* Slippery hydrophilic radiative cooling surfaces for optimal dew condensation and collection. *Commun Mater* (2026). https://doi.org/10.1038/s43246-026-01318-3

Xin Huang, Shuwang Wu, Jyotirmoy Mandal, Aryan Zaveri, Pengju Shi, Ximin He & Aaswath P. Raman

We are providing an unedited version of this manuscript to give early access to its findings. Before final publication, the manuscript will undergo further editing. Please note there may be errors present which affect the content, and all legal disclaimers apply.

If this paper is publishing under a Transparent Peer Review model then Peer Review reports will publish with the final article.

Slippery hydrophilic radiative cooling surfaces for optimal dew condensation and collection

Xin Huang[1], Shuwang Wu[1], Jyotirmoy Mandal[1], Aryan Zaveri[1], Pengju Shi[1], Ximin He[1,2] and Aaswath P. Raman[1,2*]

[1]Department of Materials Science and Engineering, University of California, Los Angeles, Los Angeles, CA 90095, USA
[2]California NanoSystems Institute, University of California, Los Angeles, Los Angeles, CA 90095, USA

*Corresponding Author: aaswath@ucla.edu

Abstract

Atmospheric water harvesting is a promising approach for potable water generation, particularly in dry landlocked environments, but high energy costs for condensation and capture remain a fundamental impediment. Passive radiative cooling offers an attractive alternative, cooling surfaces below the dew point without active energy input. However, experimental performance has been limited, with both condensation and collection of dew on radiative cooling surfaces remaining challenging. Here, we introduce a slippery hydrophilic radiative cooling surface that through its high infrared emissivity enables effective sub-ambient cooling, and through its surface wettability optimizes both condensation and collection of atmospheric water. In addition, we demonstrate a vertically oriented device architecture that allows for optimizing convection, collecting 25 g/m² of atmospheric water over 6 hours of outdoor nighttime testing at relative humidities of 65% and 45 g/m²/h at relative humidities of 95%. We also develop a model that accurately predicts system performance and show that our approach enables water generation and collection approaching the thermodynamic limit of radiative cooling-driven dew condensation. These results highlight the potential of passive radiative cooling as a practical, cost-effective technology for water generation worldwide.

Keywords: Atmospheric water harvesting, radiative cooling, slippery hydrophilic surfaces

Introduction

Water scarcity is one of the most pressing challenging issues facing humankind this century. Over fifty percent of the global population faces a shortage of water today, with that number expected to reach two-thirds by 2025[1,2]. Although desalination can facilitate the use of sea water, landlocked places are unable to take advantage of this approach to fresh water generation. Atmospheric water harvesting has thus attracted great attention for potable freshwater generation because of its ease of access and the exceptional scale of freshwater resources accessible in our atmosphere[3] .

Current atmospheric water harvesting methods are typically driven by active refrigeration, exploiting a cooled surface to cool the air below dew point powered by electricity[4,5]. However, because of the large enthalpy of condensation, active cooling methods impose large electricity requirements which are unfavorable from both a cost and carbon emissions point of view. Instead of cooling the surface to increase the local relative humidity, a significant body of research has explored atmospheric water harvesting materials with the ability to passively extract water vapor from air spontaneously such as hygroscopic materials[6–8] , silica gels[9–11] and zeolites[12–14]. However, the performance of these approaches is limited due to the energy needed to release the stored water because of the high affinity between the water and the harvesting material. A related approach that has proven very successful has been the use of metal organic framework (MOF)-based materials[15–17] that have been shown to take up water at a relatively low RH and release water with small temperature increase through tailored material modifications. However, most viable MOFs have been challenging to synthesize on a commercial scale, limiting their potential for large-scale, cost-effective water production. Furthermore, the long-term stability through cycling, as well as shaping/processing of MOFs remain potential limitations to their wider deployment[3].

With a view towards overcoming the energy constraints associated with condensing atmospheric water vapor, and building on developments in passive radiative cooling[18–27]dew condensation on radiatively-cooled surfaces has been investigated over the last several decades[16–19]. In this approach, sky-facing surfaces radiate their heat as thermal radiation into cold space through an atmospheric window in the long-wave infrared part of the electromagnetic spectrum between 8–13 μm. The cooling effect cools down the surface to below the dew point thereby facilitating condensation. Due to its underlying mechanism, passive condensation can in principle be achieved in a broad range of weather conditions, in a very simple and cost-effective manner. Recently, through proper spectral engineering, a range of high emittance radiative cooling materials[20,22,28–30] have been demonstrated, including a low-cost, high emittance radiative cooler that experimentally achieved a 11 °C temperature drop[29].

Although dew condensation through radiative cooling has been experimentally explored[31,32] with a range of materials chosen for their optical properties, comparatively little attention has been paid to the surface properties of the radiative cooling surface to facilitate both condensation and collection of generated water. For condensation applications, the water droplet usually attaches on the surface and can require additional work to efficiently remove the droplet. To that end, engineering surfaces with water nucleation and removal attracted much attention[33,34]. Recent work used a hydrophilic Al foil as the condenser to increase the condensation efficiency[35]. However strong adhesion between water and the Al foil surface makes it challenging to collect the condensed water, necessitating a weighing approach to infer the actual water condensed. For highly saturated vapors (relative humidities > 95%), another recent paper demonstrated the utility of superhydrophobic coatings[36] which can achieve self-removal of harvested dew through its strongly repelling water characteristics. While intriguing, these recent works focused on condensing vapor from a separate source, typically involving high relative humidities in the introduced water vapor. By contrast, for general atmospheric water generation, the surface requires both high water condensation efficiency as well as high water removal efficiency, which previous works have not demonstrated. Indeed, hydrophilic surfaces will typically have a high condensation rate while hydrophobic surfaces can facilitate high water removal efficiency. A potential solution to this challenge lies in the recent development of slippery liquid-infused porous surfaces (SLIPS)[37–42] consisting of a film of lubricating liquid locked in place by a micro/nanoporous substrate because of capillary action or (LISs) with lubricant infused surfaces[43,44]. Although SLIPS have shown exceptional high water condensation efficiency and water collection efficiency at the same time, in the context of water harvesting they have only been used for fog harvesting.

In this article, we experimentally develop and demonstrate high-efficiency atmospheric water harvesting driven by hydrophilic slippery radiative cooling surfaces (SRCs) that optimize both water nucleation and removal functions. We fabricate a hydrophilic slippery radiative cooling surface by incorporating the hydroxy PDMS-25 oil into the hierarchically porous poly(vinylidene fluoride-co-hexafluoropropene(P(VdF-HFP). To further increase the water collection efficiency, we optimize our system with a vertical surface, allowing water collection on both sides of the surface. We experimentally demonstrate collection of 25 g/m^2 atmospheric water over 6h of outdoor nighttime testing at relative humidities (RH of 65%, with collection as high as 45 $g/m^2/h$ water at RH of 95%. Furthermore, by optimizing the convective heat transfer coefficient in our experimental apparatus we show that our performance approaches the thermodynamic limit of performance. Our results suggest that dew condensation via radiative cooling, in addition to being of scientific interest, holds the potential to be a practical technology for water harvesting.

System design and working principle

Conventional approaches to dew condensation enabled by radiative cooling have utilized a flat or tilted sky-facing surface. However, in addition to condensing the water, a critical function needed for any real-world atmospheric water harvesting technology has been thus far ignored: collection. In prior work, droplets typically remain immobile on the surface and are manually collected by mechanical means at the end of a fixed time period. Thus prior experimental work has not achieved the performance potential that theoretical models suggest should be possible using radiative cooling. Motivated by this challenge, we introduce multi-functional hydrophilic slippery radiative cooling surfaces (SRCs). By radiatively cooling themselves, the SRCs passively cools down below the ambient air around the surfaces, which in turn, leads to condensation on the surfaces. The hydrophilic nature of the surface promotes water condensation, while its slippery nature optimizes collection by facilitating the immediate removal of condensed droplets (Fig. 1A).

Fig. 1B presents the specific steps involved in making the slippery radiative cooling surface. We first create a precursor solution of P(VdF-HFP) (polymer) and water (non-solvent) in acetone based on a phase-inversion process[20] to create a hierarchically porous polymer. We then place the film on a substrate and let it dry in open air. The acetone evaporates quickly, causing the P(VdF-HFP) to phase-separate from the water, forming micro- and nanodroplets. After the water further evaporates, the porous P(VdF-HFP) coating is created, as is shown in Fig 2A. Finally, hydroxy-terminated PDMS oil was impregnated into the porous P(VdF-HFP) surface. The sample was subsequently placed in a vacuum desiccator overnight to make sure that the PDMS oil spread uniformly on the whole substrate through capillary wicking, with excess oil removed by gravity.

The nucleation process was not considered in the design of the first liquid-infused surfaces, which were created to reduce pinning forces and produce super-liquid repellency by using non-polar liquids, such as ketones[37]. Although SLIPS has attracted significant attention over the last decade, the focus has primarily been on using hydrophobic, not hydrophilic, oil lubricants such as silicone oil[45] and Krytox oil[37,46]. However, to maximize dew condensation, hydrophilic surfaces are desirable. Thus to increase nucleation, we used a hydrophilic hydroxy-terminated PDMS oil impregnated into the porous P(VdF-HFP) thereby creating a hydrophilic slippery radiative cooling surface (SRC). While its hydrophilic nature maximizes nucleation, because of the minimized pinning force, condensed droplets are shed from the vertically-oriented surface by gravity when they reach a particular diameter.

To test this effect, and to benchmark the performance of the developed hydrophilic SRCs, we also fabricated three other reference radiative cooling water harvesting surfaces: slippery hydrophobic surfaces made of hydrophobic PDMS oil on porous P(VdF-HFP) slippery surface; non-slippery hydrophobic porous P(VdF-HFP) as well as a non-slippery hydrophilic cellulose acetate sheet. As is shown in Fig 2C, the measured static contact angle ranges from 105° for the hydrophobic porous P(VdF-HFP) and 65° for the hydrophilic SRCs. The contact angles of the hydrophobic SRCs and the hydrophilic cellulose acetate sheet are 95° and 70° respectively. We further measured the hemispherical emittance of the four samples. Instead of static contact angle dynamic contact angle effects has been also measured. As is shown in table 1, the measured CAH of hydrophilic SRCs and hydrophobic SRCs are 2.1 and 2.5 separately, while CAH of non-slippery hydrophobic porous P(VdF-HFP) is 7.4 and non-slippery hydrophilic cellulose acetate sheet is 43.1. As is shown in Fig 2B, all of them have high hemispherical emittance, ranging from 0.93-0.97, indicating suitability for dew condensation from a radiative cooling perspective.

We first assessed condensation behavior of the four developed materials in a controlled lab environment. Four samples were attached on the same thermoelectric cooler set to 5℃ below the dew point indoors with the results shown in Fig 2D. For the reference non-slippery hydrophobic P(VdF-HFP) and hydrophilic cellulose surfaces, the water droplets that form are pinned to the surface with many tiny droplets forming but not able to coalesce or roll down. On the hydrophobic SRC the droplets that form are very mobile, resulting in dynamic coalescence into larger droplets. However droplet nucleation is greatly limited due to the hydrophobic nature of the surface. By contrast, there are numerous nucleation sites visible on the hydrophilic SRCs, and the droplets are quite mobile, which makes the maximum droplet size of the hydrophilic SRCs orders of magnitude larger than the other three samples. On the hydrophilic SRCs, rapid droplet coalescence can efficiently increase the droplet volume over time, favoring fast droplet removal by gravity.

Sample	Hydrophobic RCs	Hydrophilic RCs	Hydrophobic SRCs	Hydrophilic SRCs
Advancing angle	94.4°	94.5°	100.3°	82.6°
receiving angle	87°	51.4°	97.8°	80.5°
CAH	7.4	43.1	2.5	2.1

Table 1: CAH comparison of four samples, hydrophobic material, hydrophilic material, hydrophobic SRCs, hydrophilic SRCs.

We next quantified the atmospheric water harvesting capabilities of the four materials, with a particular focus on not only assessing total water condensed, but also the amount that one could collect, particularly with the SRCs. We performed outdoor experiments with each material integrated into a custom-built apparatus shown in Fig. 3A. The samples were mounted vertically with a plastic holder to allow for water vapor condensation on both sides of the surface. The vertical orientation facilitated collection by gravity into a collection chamber beneath. This is an important design development that allows for the practical utilization of radiative cooling for dew condensation, as, for the first time, no manual or mechanical removal of water is needed. Two aluminized Mylar mirrors, at a 45° angle relative to the ground, were used to reflect the thermal radiation of the vertically oriented radiative cooling surfaces to the sky, facilitating sub-ambient radiative cooling. We demonstrated the performance of the atmospheric water collecting at a test site at the University of California, Los Angeles, (location shown in Fig. 3B), by placing the four samples into four identical apparatuses during night-time hours and testing their performance.

As shown in the temperature data of Fig. 3C, immediately after the samples are exposed to the environment and sky, a temperature drop of 4-6℃ below ambient temperature is achieved, a signature of sub-ambient radiative cooling. We note however that the hydrophilic SRC reaches a steady-state temperature 0.5~1 ℃ higher than the other three materials. Given the nearly identical emittance of all the materials and apparatus design, this temperature difference is indicative of the latent heat of condensation arising from the higher condensation rate on the hydrophilic SRC surface. This hypothesis is verified in Fig. 3D, which summarizes the final collected yield of these four materials in identical apparatuses. For the non-slipper hydrophobic P(VdF-HFP) and hydrophilic cellulose acetate materials, the condensed water droplets remain pinned to the surface, leading to near-zero collection during the six hours of testing.

To assess the volume of water condensed on these surfaces we use a napkin to mechanically wipe the surfaces and measure the weight difference before and after to get the condensation yield. By contrast, for the hydrophobic and hydrophilic SRCs, the condensed water droplets drop easily by gravity and were successfully collected in the bottom container without any other mechanical force needed. For relative humidities ranging from 62% to 74% during this night of testing, the slippery hydrophilic radiative cooling surfaces collected 0.5 mL of water with a 0.02 m^2 radiative cooling surface in 6 hours.

We carried out additional experiments in different weather conditions with relative humidities ranging from 68% to 87%. The temperature of these four samples is shown in Fig. 3E. Because of the higher humidities the samples experience a more modest temperature drop of 3-5 ℃ below ambient temperature, since higher atmospheric moisture reduces the net cooling powers and steady-state temperatures achievable by radiative cooling. However, because of the higher humidity (and the elevated dew point) more water vapor is available around the radiative cooler leading to a larger yield, as is shown in Fig. 3F. For the non-slippery hydrophobic P(VdF-HFP) and hydrophilic cellulose acetate, although more water droplets form on the surface, the pinning effect still prevents them dropping to the bottom container. Therefore, for hydrophobic P(VdF-HFP) and hydrophilic cellulose acetate, the result in Fig. 3F shows the condensation yield which comes from the weight difference of the napkin before and after mechanically wiping the surface. As with the previous experiment, the slippery hydrophilic surface performs exceptionally well, yielding by far the largest collection yield of 1.5 mL over 6 hours of testing.

The convective heat transfer coefficient experienced by the radiative cooling surface is another important parameter affecting atmospheric water collection by radiative cooling. A smaller heat transfer coefficient leads to a colder radiative cooling surface because of smaller heat loss to the environment. The cooler surface would be able to more effectively condense water vapor, even in an arid environment. However, a lower convective heat transfer coefficient by definition implies that less water vapor will flow past the radiatively cooled surface, thereby resulting in less condensate forming on the surface. Thus, as has previously been noted in the literature, there is an optimal heat transfer coefficient for atmospheric water collection driven by radiative cooling[47].

To test this effect, we prepared three identical hydrophilic SRCs with the apparatus design shown in Fig. 3A, but modified the permeability of the front wind covers of each of them. As is shown in Fig. 4A, the first surface is directly exposed to the ambient air without any cover, representing the largest convective heat transfer coefficient scenario. The second sample was encapsulated with the low density polyethylene (LDPE[48]) as in our previous experiments (Fig. 3), representing a low heat transfer coefficient scenario. Finally, we created a partially insulated cover by introducing a random set of air holes into the LDPE cover, representing an intermediate heat transfer coefficient scenario that we hypothesized might yield a higher dew yield than the other two scenarios we considered. The experimentally measured temperatures of these three setups are shown in Fig. 4B. By virtue of having the smallest heat transfer coefficient, the sample fully closed with LDPE reaches the lowest temperature, but it collects very little water, as shown in Fig. 4C. For the largest heat transfer coefficient, which is the scenario where the sample directly contacts the air, the higher surface temperature limits its atmospheric water collection even though this scenario also yields the largest flow of air moisture by the sample. As is shown in Fig. 4C, the highest atmospheric water collection comes from the partially open setup with an estimated heat transfer coefficient that is significantly closer to the ideal heat transfer coefficient. Notably the partially open setup yields a collected dew yield 50% higher (a value of 120 g/m^2/night) than the open setup used in our previous experiments. This significant performance enhancement has not previously been demonstrated in the literature to the best of our knowledge.

We next use a theoretical model for radiative cooling atmospheric water harvesting to predict the freshwater yield[47] and compare against our achieved performance (see Supplementary Information). The theoretical limit, at the optimal convective heat transfer coefficient, as a function of relative humidity is plotted as a dashed line in Fig. 5A. Experimental atmospheric water collection results of these four samples at different relative humidity values are also plotted in Fig. 5A. As might be intuitively expected, increasing relative humidity favors the atmospheric water harvesting yield. Remarkably, our hydrophilic SRCs outperform the other three materials for all humidities and achieve collection rates very close to the theoretical limits. A key advantage of the hydrophilic SRC is that the hydrophilic oil surface attracts water vapor condensing on the surface because of larger numbers of nucleation sites[38]. Moreover, the slippery surface favors rapid droplet removal by gravitation once the water droplet reaches a critical size. Furthermore, the fast droplet removal will recover the nucleation sites covered by the liquid droplet and increase condensation efficiency.

Next, we compare the performance achieved by the apparatuses shown in Fig. 4 with varying convective heat transfer coefficients against the theoretical model. Fig. 5B shows the freshwater atmospheric water production with the theoretical model against experiment at different heat transfer coefficients. At a particular temperature and relative humidity, there is an optimal heat transfer coefficient to maximize atmospheric water collection. To benchmark our systems against the model's predicted limits we develop a simple heuristic model for the expected convective heat transfer coefficients of our apparatuses. We expect our open system to have a convective heat transfer coefficient ranging from 7 W m^{-2} K^{-1} to 11 W m^{-2} K^{-1}, the closed system a heat transfer coefficient between 0.2 W m^{-2} K^{-1} to 1 W m^{-2} K^{-1} and the partially open system a heat transfer coefficient ranging from 2 W m^{-2} K^{-1} to 6 W m^{-2} K^{-1}. We note here that our partially open setup achieves a performance near the highest possible dew condensation rate predicted by the theoretical model. From Fig. 5B, we can see that our hydrophilic radiative cooling slippery surfaces achieve exceptional performance near the limits of what is possible.

Conclusion

To summarize, we have developed slippery hydrophilic radiative cooling surface and highlighted the remarkable atmospheric water collecting performance they make possible. Compared with other atmospheric water harvesting methods, our approach is passive, simple and uses low-cost materials. It is able to achieve high water condensation efficiency as well as excellent water self-removal and collection. Furthermore, we emphasize that we could push this technology to the theoretical thermodynamic limit by optimizing the convective heat transfer coefficient of the apparatus used. Our preliminary results to that end indicate performance near the theoretical limit has already been achieved by our material and apparatus. While radiative cooling has emerged as an important field for research in energy challenges in recent years, our results emphasize the critical role that exploiting the thermodynamic resource of space cold could have in addressing the water challenges we face this century.

Acknowledgments

This material was based upon work supported by the National Science Foundation under grant no. ECCS-2146577

Data Availability Statement

All data is available upon request to the authors.

Author Contributions

A.R. and X. Huang developed the concept. X. Huang designed and fabricated the materials and conducted the indoor and outdoor experiments. S.W. and P.S. performed indoor wettability and condensation studies with X. He providing supervision. J.M. and A.Z. assisted with modeling and experimental design. A.R. supervised the project. A.R. and X. Huang wrote the manuscript with all authors reviewing and editing the final version.

Disclosure Statement

The authors declare no competing interests or disclosures.

References

1. Zhuang, S., Qi, H., Wang, X., Li, X., Liu, K., Liu, J., and Zhang, H. (2021). Advances in Solar-Driven Hygroscopic Water Harvesting. Global Challenges *5*, 2000085. https://doi.org/10.1002/gch2.202000085.

2. Mekonnen, M.M., and Hoekstra, A.Y. Four billion people facing severe water scarcity. Science Advances *2*, e1500323. https://doi.org/10.1126/sciadv.1500323.

3. Zhou, X., Lu, H., Zhao, F., and Yu, G. (2020). Atmospheric Water Harvesting: A Review of Material and Structural Designs. ACS Materials Lett. *2*, 671–684. https://doi.org/10.1021/acsmaterialslett.0c00130.

4. Wikramanayake, E.D., Ozkan, O., and Bahadur, V. (2017). Landfill gas-powered atmospheric water harvesting for oilfield operations in the United States. Energy *138*, 647–658. https://doi.org/10.1016/j.energy.2017.07.062.

5. Wahlgren, R.V. (2001). Atmospheric water vapour processor designs for potable water production: a review. Water Research *35*, 1–22. https://doi.org/10.1016/S0043-1354(00)00247-5.

6. Zhang, H., Yoshino, H., Hasegawa, K., Liu, J., Zhang, W., and Xuan, H. (2017). Practical moisture buffering effect of three hygroscopic materials in real-world conditions. Energy and Buildings *139*, 214–223. https://doi.org/10.1016/j.enbuild.2017.01.021.

7. Kallenberger, P.A., and Fröba, M. (2018). Water harvesting from air with a hygroscopic salt in a hydrogel–derived matrix. Commun Chem *1*, 1–6. https://doi.org/10.1038/s42004-018-0028-9.

8. Li, R., Shi, Y., Alsaedi, M., Wu, M., Shi, L., and Wang, P. (2018). Hybrid Hydrogel with High Water Vapor Harvesting Capacity for Deployable Solar-Driven Atmospheric Water Generator. Environ. Sci. Technol. *52*, 11367–11377. https://doi.org/10.1021/acs.est.8b02852.

9. Wang, D.C., Xia, Z.Z., Wu, J.Y., Wang, R.Z., Zhai, H., and Dou, W.D. (2005). Study of a novel silica gel–water adsorption chiller. Part I. Design and performance prediction. International Journal of Refrigeration *28*, 1073–1083. https://doi.org/10.1016/j.ijrefrig.2005.03.001.

10. Ng, K.C., Chua, H.T., Chung, C.Y., Loke, C.H., Kashiwagi, T., Akisawa, A., and Saha, B.B. (2001). Experimental investigation of the silica gel–water adsorption isotherm characteristics. Applied Thermal Engineering *21*, 1631–1642. https://doi.org/10.1016/S1359-4311(01)00039-4.

11. Zhuravlev, L.T. (2000). The surface chemistry of amorphous silica. Zhuravlev model. Colloids and Surfaces A: Physicochemical and Engineering Aspects *173*, 1–38. https://doi.org/10.1016/S0927-7757(00)00556-2.

12. Trzpit, M., Soulard, M., Patarin, J., Desbiens, N., Cailliez, F., Boutin, A., Demachy, I., and Fuchs, A.H. (2007). The Effect of Local Defects on Water Adsorption in Silicalite-1 Zeolite: A Joint Experimental and Molecular Simulation Study. Langmuir *23*, 10131–10139. https://doi.org/10.1021/la7011205.

13. Jänchen, J., Ackermann, D., Stach, H., and Brösicke, W. (2004). Studies of the water adsorption on Zeolites and modified mesoporous materials for seasonal storage of solar heat. Solar Energy *76*, 339–344. https://doi.org/10.1016/j.solener.2003.07.036.

14. Wei, X., Wang, W., Xiao, J., Zhang, L., Chen, H., and Ding, J. (2013). Hierarchically porous aluminosilicates as the water vapor adsorbents for dehumidification. Chemical Engineering Journal *228*, 1133–1139. https://doi.org/10.1016/j.cej.2013.05.062.

15. Kalmutzki, M.J., Diercks, C.S., and Yaghi, O.M. (2018). Metal–Organic Frameworks for Water Harvesting from Air. Advanced Materials *30*, 1704304. https://doi.org/10.1002/adma.201704304.

16. Kim, H., Yang, S., Rao, S.R., Narayanan, S., Kapustin, E.A., Furukawa, H., Umans, A.S., Yaghi, O.M., and Wang, E.N. (2017). Water harvesting from air with metal-organic frameworks powered by natural sunlight. Science *356*, 430–434. https://doi.org/10.1126/science.aam8743.

17. Dietzel, P.D.C., Johnsen, R.E., Blom, R., and Fjellvåg, H. (2008). Structural Changes and Coordinatively Unsaturated Metal Atoms on Dehydration of Honeycomb Analogous Microporous Metal–Organic Frameworks. Chemistry – A European Journal *14*, 2389–2397. https://doi.org/10.1002/chem.200701370.

18. Raman, A.P., Anoma, M.A., Zhu, L., Rephaeli, E., and Fan, S. (2014). Passive radiative cooling below ambient air temperature under direct sunlight. Nature *515*, 540–544. https://doi.org/10.1038/nature13883.

19. Chen, Z., Zhu, L., Raman, A., and Fan, S. (2016). Radiative cooling to deep sub-freezing temperatures through a 24-h day–night cycle. Nat Commun *7*, 13729. https://doi.org/10.1038/ncomms13729.

20. Mandal, J., Fu, Y., Overvig, A.C., Jia, M., Sun, K., Shi, N.N., Zhou, H., Xiao, X., Yu, N., and Yang, Y. (2018). Hierarchically porous polymer coatings for highly efficient passive daytime radiative cooling. Science *362*, 315–319. https://doi.org/10.1126/science.aat9513.

21. Trombe, F. (1967). Perspectives sur l'utilisation des rayonnements solaires et terrestres dans certaines re´gions du monde. Revue Generale Thermique *6*, 1215–1234.

22. Berdahl, P. (1984). Radiative cooling with MgO and/or LiF layers. Appl. Opt., AO *23*, 370–372. https://doi.org/10.1364/AO.23.000370.

23. Raman, A.P., Li, W., and Fan, S. (2019). Generating Light from Darkness. Joule *3*, 2679–2686. https://doi.org/10.1016/j.joule.2019.08.009.

24. Bhatia, B., Leroy, A., Shen, Y., Zhao, L., Gianello, M., Li, D., Gu, T., Hu, J., Soljačić, M., and Wang, E.N. (2018). Passive directional sub-ambient daytime radiative cooling. Nat Commun *9*, 5001. https://doi.org/10.1038/s41467-018-07293-9.

25. Granqvist, C.G., and Hjortsberg, A. (1981). Radiative cooling to low temperatures: General considerations and application to selectively emitting SiO films. Journal of Applied Physics *52*, 4205–4220. https://doi.org/10.1063/1.329270.

26. Hossain, M.M., and Gu, M. (2016). Radiative Cooling: Principles, Progress, and Potentials. Advanced Science *3*, 1500360. https://doi.org/10.1002/advs.201500360.

27. Zhao, D., Aili, A., Zhai, Y., Xu, S., Tan, G., Yin, X., and Yang, R. (2019). Radiative sky cooling: Fundamental principles, materials, and applications. Applied Physics Reviews *6*, 021306. https://doi.org/10.1063/1.5087281.

28. Mandal, J., Yang, Y., Yu, N., and Raman, A.P. (2020). Paints as a Scalable and Effective Radiative Cooling Technology for Buildings. Joule *4*, 1350–1356. https://doi.org/10.1016/j.joule.2020.04.010.

29. Huang, X., Mandal, J., and Raman, A. (2021). Do-it-yourself radiative cooler as a radiative cooling standard and cooling component for device design. JPE *12*, 012112. https://doi.org/10.1117/1.JPE.12.012112.

30. Gentle, A.R., and Smith, G.B. (2015). A Subambient Open Roof Surface under the Mid-Summer Sun. Advanced Science *2*, 1500119. https://doi.org/10.1002/advs.201500119.

31. Muselli, M., Beysens, D., Mileta, M., and Milimouk, I. (2009). Dew and rain water collection in the Dalmatian Coast, Croatia. Atmospheric Research *92*, 455–463. https://doi.org/10.1016/j.atmosres.2009.01.004.

32. Muselli, M., Beysens, D., Marcillat, J., Milimouk, I., Nilsson, T., and Louche, A. (2002). Dew water collector for potable water in Ajaccio (Corsica Island, France). Atmospheric Research *64*, 297–312. https://doi.org/10.1016/S0169-8095(02)00100-X.

33. Liu, X., Trosseille, J., Mongruel, A., Marty, F., Basset, P., Laurent, J., Royon, L., Cui, T., Beysens, D., and Bourouina, T. (2021). Tailoring silicon for dew water harvesting panels. iScience *24*, 102814. https://doi.org/10.1016/j.isci.2021.102814.

34. Beysens, D., and Muselli, M. (2024). Emerging Water Recovery Processes from Dew and Light Rain. In Clean Water: Next Generation Technologies, K. Jlassi, M. A. Oturan, A. F. Ismail, and M. M. Chehimi, eds. (Springer International Publishing), pp. 1–24. https://doi.org/10.1007/978-3-031-48228-1_1.

35. Zhou, M., Song, H., Xu, X., Shahsafi, A., Qu, Y., Xia, Z., Ma, Z., Kats, M.A., Zhu, J., Ooi, B.S., et al. (2021). Vapor condensation with daytime radiative cooling. PNAS *118*. https://doi.org/10.1073/pnas.2019292118.

36. Haechler, I., Park, H., Schnoering, G., Gulich, T., Rohner, M., Tripathy, A., Milionis, A., Schutzius, T.M., and Poulikakos, D. (2021). Exploiting radiative cooling for uninterrupted 24-hour water harvesting from the atmosphere. Science Advances *7*, eabf3978. https://doi.org/10.1126/sciadv.abf3978.

37. Wong, T.-S., Kang, S.H., Tang, S.K.Y., Smythe, E.J., Hatton, B.D., Grinthal, A., and Aizenberg, J. (2011). Bioinspired self-repairing slippery surfaces with pressure-stable omniphobicity. Nature *477*, 443–447. https://doi.org/10.1038/nature10447.

38. Dai, X., Sun, N., Nielsen, S.O., Stogin, B.B., Wang, J., Yang, S., and Wong, T.-S. (2018). Hydrophilic directional slippery rough surfaces for water harvesting. Sci. Adv. *4*, eaaq0919. https://doi.org/10.1126/sciadv.aaq0919.

39. Feng, R., Xu, C., Song, F., Wang, F., Wang, X.-L., and Wang, Y.-Z. (2020). A Bioinspired Slippery Surface with Stable Lubricant Impregnation for Efficient Water Harvesting. ACS Appl. Mater. Interfaces *12*, 12373–12381. https://doi.org/10.1021/acsami.0c00234.

40. Guo, Z., Zhang, L., Monga, D., Stone, H.A., and Dai, X. (2021). Hydrophilic slippery surface enabled coarsening effect for rapid water harvesting. Cell Reports Physical Science *2*, 100387. https://doi.org/10.1016/j.xcrp.2021.100387.

41. Lyu, P., Zhang, X., Peng, M., Shang, B., and Liu, X. (2021). Multibioinspired Wettable Patterned Slippery Surface for Efficient Water Harvesting. Advanced Materials Interfaces *8*, 2100691. https://doi.org/10.1002/admi.202100691.

42. Samaha, M.A., and Gad-el-Hak, M. (2021). Slippery surfaces: A decade of progress. Physics of Fluids *33*, 071301. https://doi.org/10.1063/5.0056967.

43. Lavielle, N., Mongruel, A., Bourouina, T., Royon, L., and Beysens, D. (2023). Plastic foil micro-grooved by embossing enhances dew collection without aging effects. Materials Today Sustainability *24*, 100566. https://doi.org/10.1016/j.mtsust.2023.100566.

44. Hoque, M.J., Sett, S., Yan, X., Liu, D., Rabbi, K.F., Qiu, H., Qureshi, M., Barac, G., Bolton, L., and Miljkovic, N. (2022). Life Span of Slippery Lubricant Infused Surfaces. ACS Appl. Mater. Interfaces *14*, 4598–4611. https://doi.org/10.1021/acsami.1c17010.

45. Anand, S., Rykaczewski, K., Subramanyam, S.B., Beysens, D., and Varanasi, K.K. (2014). How droplets nucleate and grow on liquids and liquid impregnated surfaces. Soft Matter *11*, 69–80. https://doi.org/10.1039/C4SM01424C.

46. Sun, J., and Weisensee, P.B. (2019). Microdroplet self-propulsion during dropwise condensation on lubricant-infused surfaces. Soft Matter *15*, 4808–4817. https://doi.org/10.1039/C9SM00493A.

47. Dong, M., Zhang, Z., Shi, Y., Zhao, X., Fan, S., and Chen, Z. (2020). Fundamental Limits of the Dew-Harvesting Technology. Nanoscale and Microscale Thermophysical Engineering *24*, 43–52. https://doi.org/10.1080/15567265.2020.1722300.

48. Huang, X., Mandal, J., Xu, J., and Raman, A.P. (2022). Passive freezing desalination driven by radiative cooling. Joule *6*, 2762–2775. https://doi.org/10.1016/j.joule.2022.10.009.

Figure 1: Design of the multi-functional hydrophilic slippery radiative cooling surfaces. (A) Working principle of atmospheric water harvesting process with slippery radiative cooling surface. B) Schematics showing the fabrication of hydrophilic SRCs by infiltrating a porous solid with lubricating film.

Figure 2: Comparison of four samples, hydrophobic material, hydrophilic material, hydrophobic SRCs, hydrophilic SRCs. A) SEM image of P(VdF-HFP) showing the porous features B) Measured emittance of four samples. C) Measured contact angle of four samples D) Imaged water condensation performance of four samples.

Figure 3: A) Three-dimensional schematic of the radiative cooling apparatus. B) Photo of the setup and its surroundings at the University of California, Los Angeles, in Los Angeles, CA, USA. Experiments were conducted at night. C) Measurements of temperature of four samples, including hydrophobic, hydrophilic, hydrophobic SRCs and hydrophilic SRCs against ambient temperature on a clear night (01/03/2022). D) Experimental collection results of four samples, including hydrophobic, hydrophilic, hydrophobic SRCs and hydrophilic SRCs (measurement uncertainty +/- 5%). E) Measurements of temperature of four samples against ambient temperature on a clear night (01/04/2022). F) Experimental collection results of the four samples (measurement uncertainty +/- 5%).

Figure 4: A) Schematic of the experimental apparatus with three modified front covers: sample exposed to air directly, sample sealed with low density polyethylene film, and sample partially sealed with porous low density polyethylene film. B) Measurements of temperature of hydrophilic SRCs with three different setups against ambient temperature on a clear night at University of California on 01/05/2022. C) Experimental water collection results of three samples with the different set up in Fig. 4A highlighting that the partially open setup achieves as much as 120 g/m^2/night collection efficiency (measurement uncertainty +/- 5%).

Figure 5: Modeled freshwater atmospheric water production rates with the theoretical model against experiment. A) Effect of relative humidity. Higher relative humidities yield higher water yields, as expected, with the hydrophilic SRCs performing nearing the theoretical limits (measurement uncertainty +/- 5%). B) Effect of heat transfer coefficient. The partially open setup's water yield is near the optimal expected value, indicating the achieved performance is near the best possible value given the environmental conditions during the testing shown in Fig. 4.

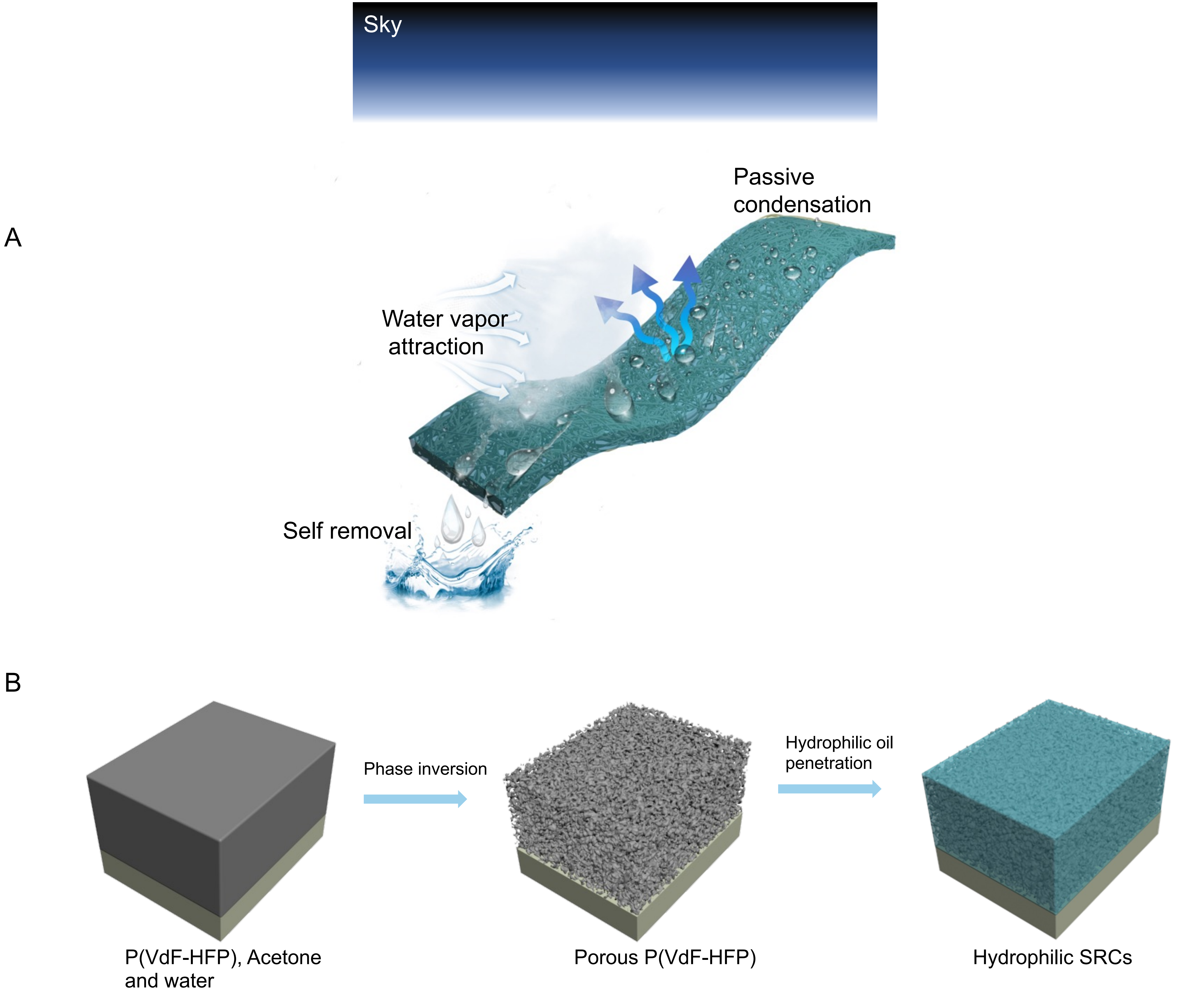
A
Sky
Passive
condensation
Water vapor
attraction
Self removal
B
Phase inversion
Hydrophilic oil
penetration
P(VdF-HFP), Acetone
and water
Porous P(VdF-HFP)
Hydrophilic SRCs

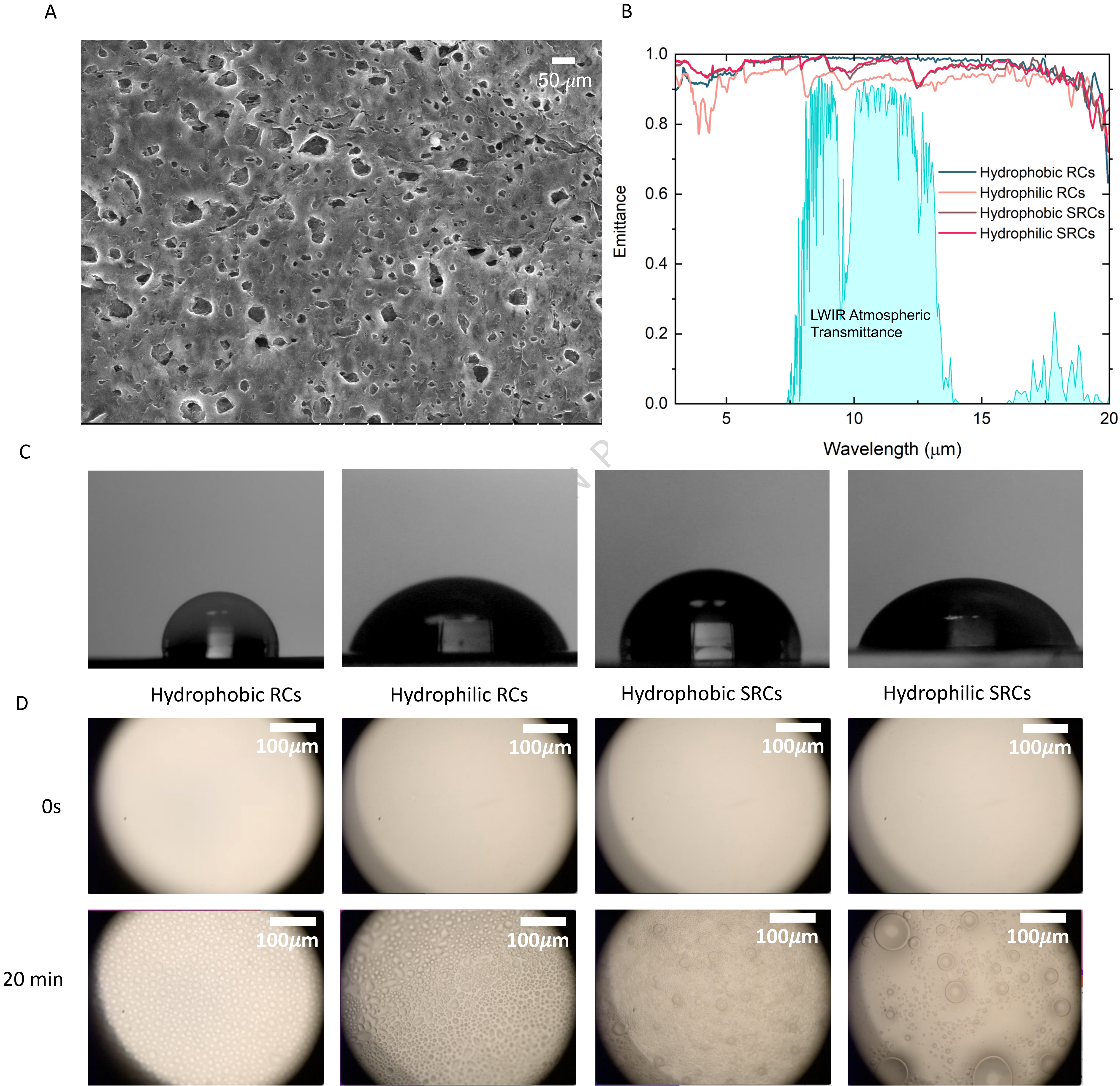
A
50 μm
B
1.0
0.8
0.6
0.4
0.2
0.0
Emittance
5
10
15
20
Wavelength (μm)
Hydrophobic RCs
Hydrophilic RCs
Hydrophobic SRCs
Hydrophilic SRCs
LWIR Atmospheric
Transmittance
C
Hydrophobic RCs
Hydrophilic RCs
Hydrophobic SRCs
Hydrophilic SRCs
D
0s
20 min
100μm

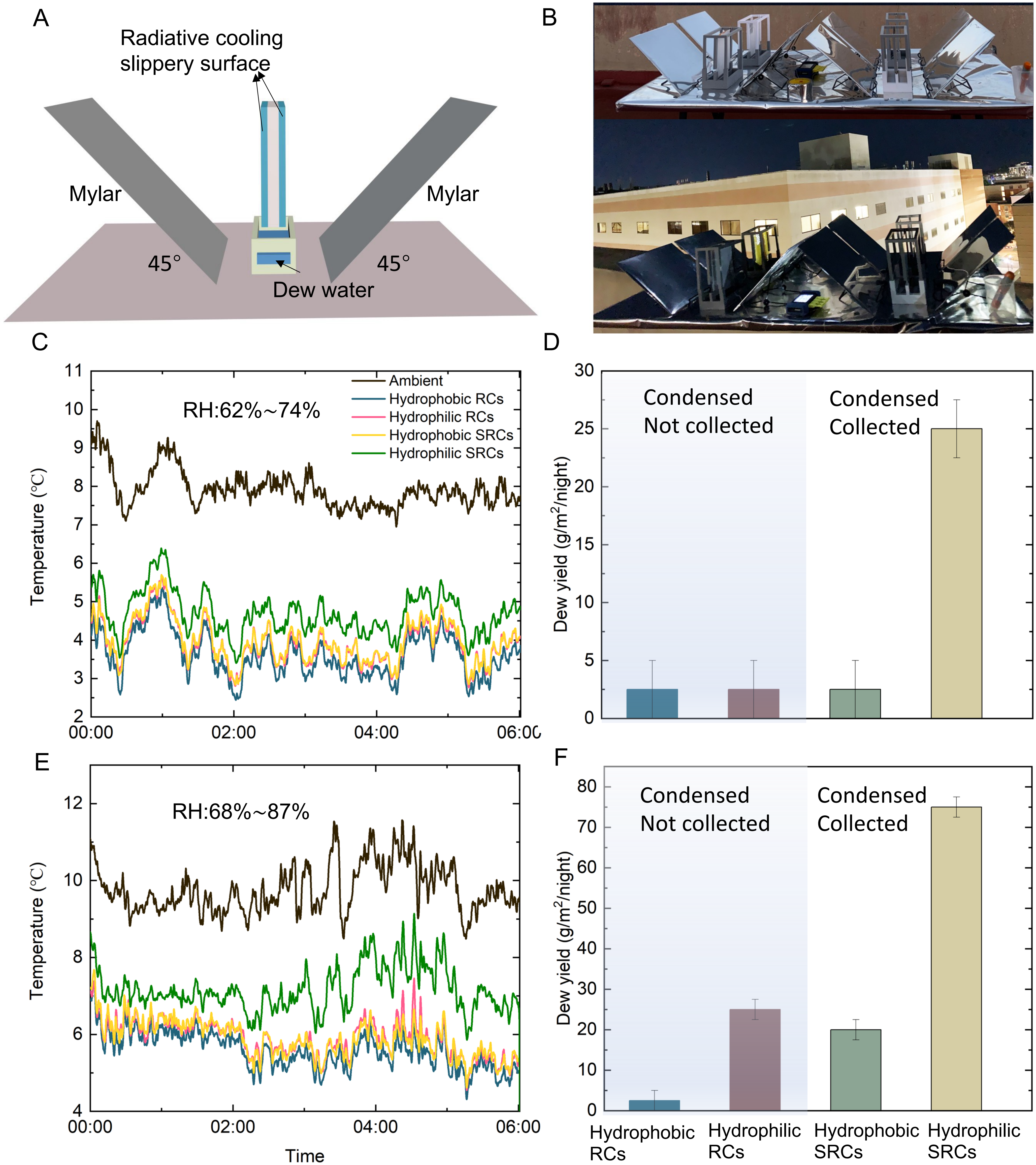

A
Radiative cooling slippery surface
Mylar
Mylar
45°
45°
Dew water
B
C
RH:62%~74%
Ambient
Hydrophobic RCs
Hydrophilic RCs
Hydrophobic SRCs
Hydrophilic SRCs
Temperature (℃)
00:00
02:00
04:00
06:00
D
Condensed Not collected
Condensed Collected
Dew yield (g/m²/night)
E
RH:68%~87%
Temperature (℃)
Time
F
Condensed Not collected
Condensed Collected
Dew yield (g/m²/night)
Hydrophobic RCs
Hydrophilic RCs
Hydrophobic SRCs
Hydrophilic SRCs

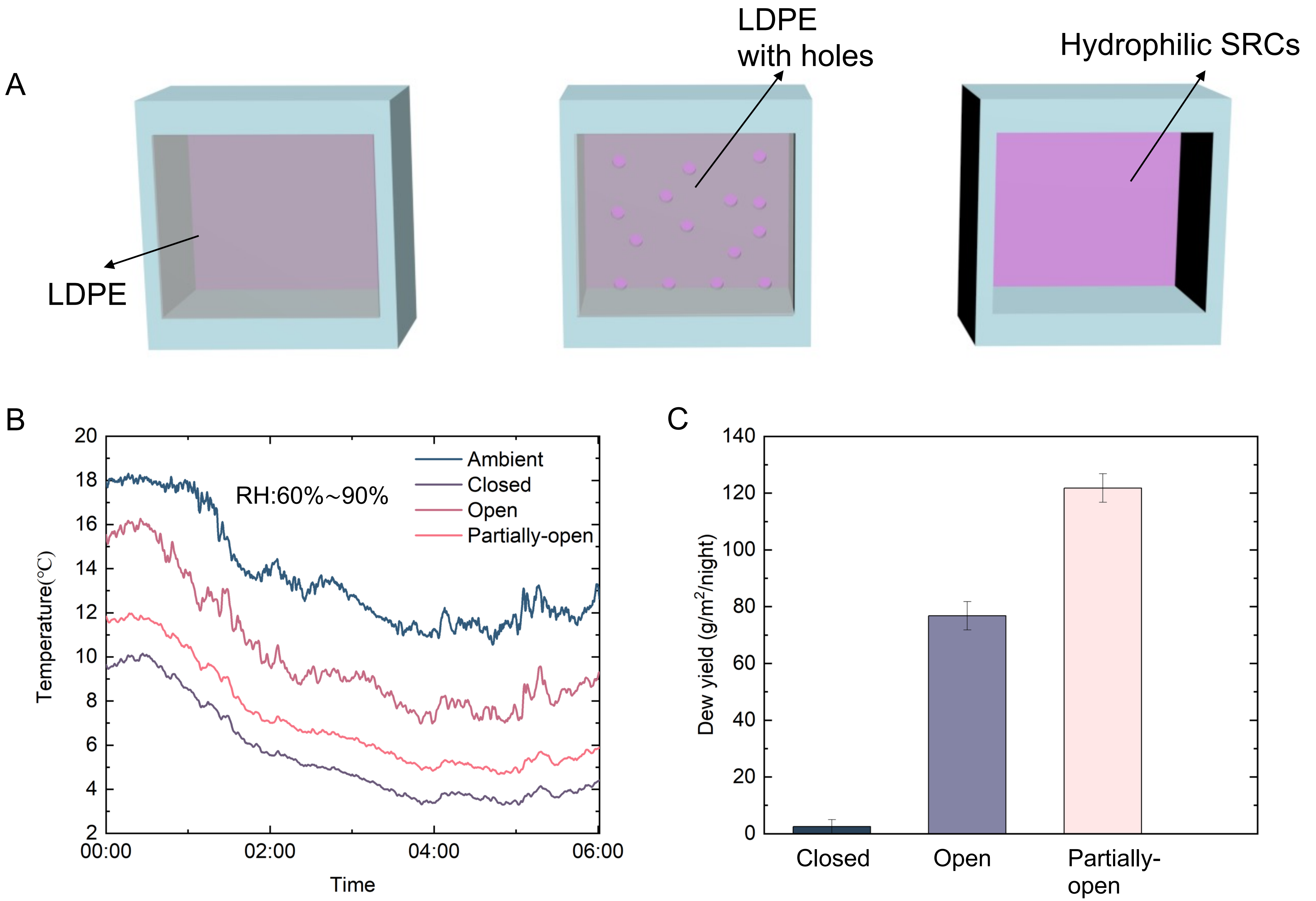
A
LDPE
LDPE
with holes
Hydrophilic SRCs
B
Temperature(℃)
RH:60%~90%
Ambient
Closed
Open
Partially-open
20
18
16
14
12
10
8
6
4
2
00:00
02:00
04:00
06:00
Time
C
Dew yield (g/m2/night)
140
120
100
80
60
40
20
0
Closed
Open
Partially-
open

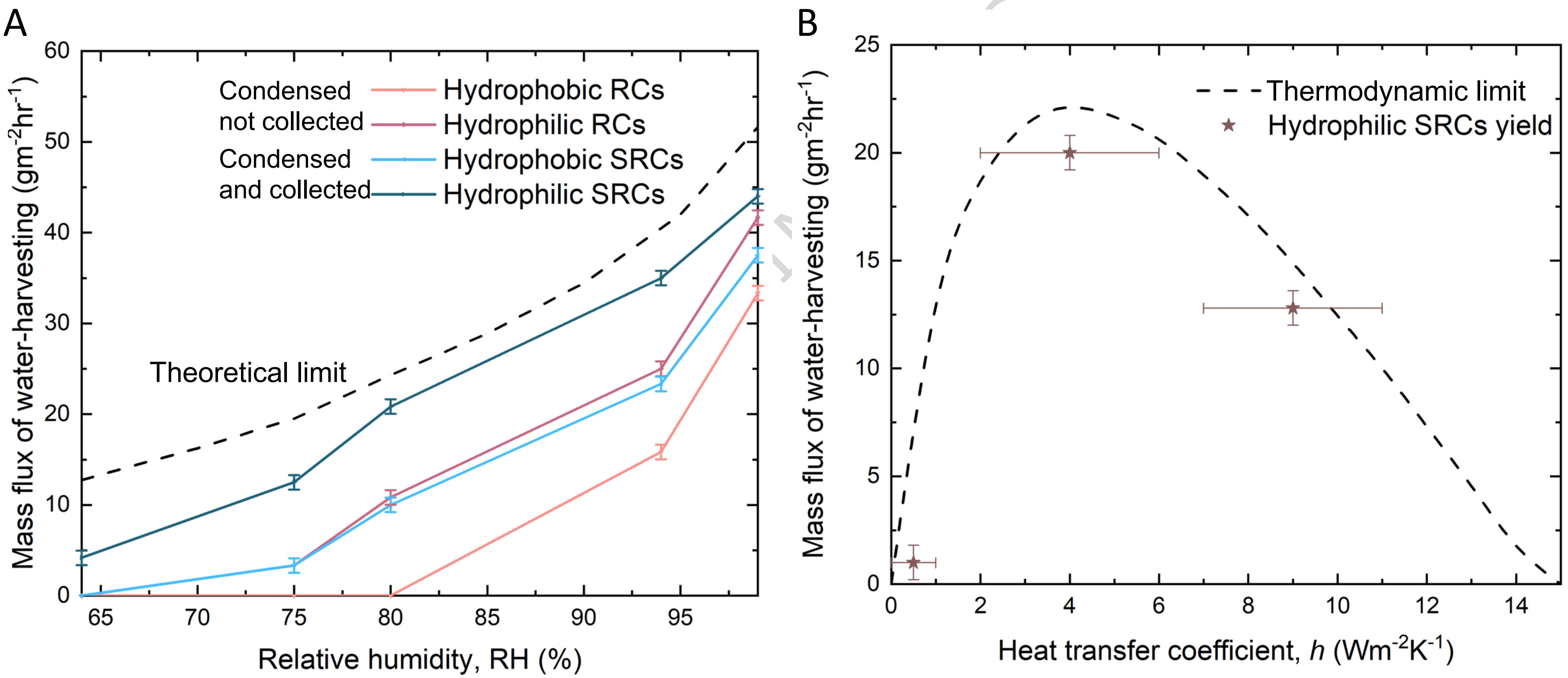
A
B
Condensed not collected
Condensed and collected
Hydrophobic RCs
Hydrophilic RCs
Hydrophobic SRCs
Hydrophilic SRCs
Theoretical limit
Mass flux of water-harvesting (gm-2hr-1)
Relative humidity, RH (%)
Thermodynamic limit
Hydrophilic SRCs yield
Heat transfer coefficient, h (Wm-2K-1)